Hindawi Publishing Corporation
EURASIP Journal on Wireless Communications and Networking
Volume 2007, Article ID 54968, 10 pages
doi:10.1155/2007/54968

Research Article

Communication Timing Control with Interference Detection for Wireless Sensor Networks

Yuki Kubo[1, 2] and Kokuke Sekiyama[3]

[1] *Ubiquitous System Laboratory, Corporate Research and Development Center, OKI Electric Industry Co., Ltd., 2-5-7 Honmachi, Chuo-Ku, Osaka-Shi, Osaka 541-0053, Japan*
[2] *Department of System Design Engineering, University of Fukui, 3-9-1 Bunkyo, Fukui-Shi, Fukui 910-8507, Japan*
[3] *Department of Micro-Nano Systems Engineering, Nagoya University, Furo-Cho, Chikusa-Ku, Nagoya 464-8603, Japan*

Received 31 May 2006; Revised 16 October 2006; Accepted 18 October 2006

Recommended by Xiuzhen Cheng

This paper deals with a novel communication timing control for wireless networks and radio interference problem. Communication timing control is based on the mutual synchronization of coupled phase oscillatory dynamics with a stochastic adaptation, according to the history of collision frequency in communication nodes. Through local and fully distributed interactions in the communication network, the coupled phase dynamics self-organizes collision-free communication. In wireless communication, the influence of the interference wave causes unexpected collisions. Therefore, we propose a more effective timing control by selecting the interaction nodes according to the received signal strength.

1. INTRODUCTION

In recent years, research on wireless sensor networks has been promoted rapidly [1]. The sensor networks are composed of distributed sensor devices connected with wireless communication and sensing functions. Potential application fields of the sensor networks include stock-management systems, road traffic surveillance systems, and air-conditioning control systems of a large-scale institution and so on. There are many technical issues in the sensor networks. In this paper, we deal with two problems. One of them is a communication timing control for collision avoidance. Another is the influence of interference wave on the communication timing control. In order to cope with malfunctions and changes of the number of active sensor nodes, a distributed autonomous communication timing control is preferable to centralized approaches which must rely on a fixed base station in general.

In order to avoid the collision issue, TDMA [2] system has been presented, which is a multiplexing technology in the time domain that makes it possible to avoid collisions by assigning a communication slot to one frame. Hence, no collision occurs, and any node can obtain impartial communication right in TDMA. TDMA is widely used in cellular telephone systems. However, TDMA is fundamentally a centralized management technique depending on a base station and is applicable to a star link network. Meanwhile, distributed slot assignment TDMA approach for ad hoc networks has been proposed. In Ephremides and Truong algorithm [3], allocation of one transmission slot is assured for each node by preparing N slots for N nodes. In addition, it is possible to add more slot allocations by referring to information of the slot allocation within the two hop nodes for the collision avoidance based on the distributed algorithm. However, this algorithm requires total number of the node. Hence, this algorithm has a limitation in changing the number of nodes flexibly. USAP-MA [4] deals with a distributed slot assignment in TDMA for changes of the number of nodes. This method provides a dynamic change of frame length corresponding to the number of nodes and network topology, and improves bandwidth efficiency. Also, the other methods of slot reservation have been proposed for TDMA [4–6]. However, these TDMA-based approaches require a global time synchronization.

As another collision avoidance technique, CSMA [7, 8] has been widely used. CSMA is a simple and scalable protocol. In the case of low-traffic situation, CSMA works efficiently. However, according to the increase of nodes, communication throughput sharply declines due to occurrence of

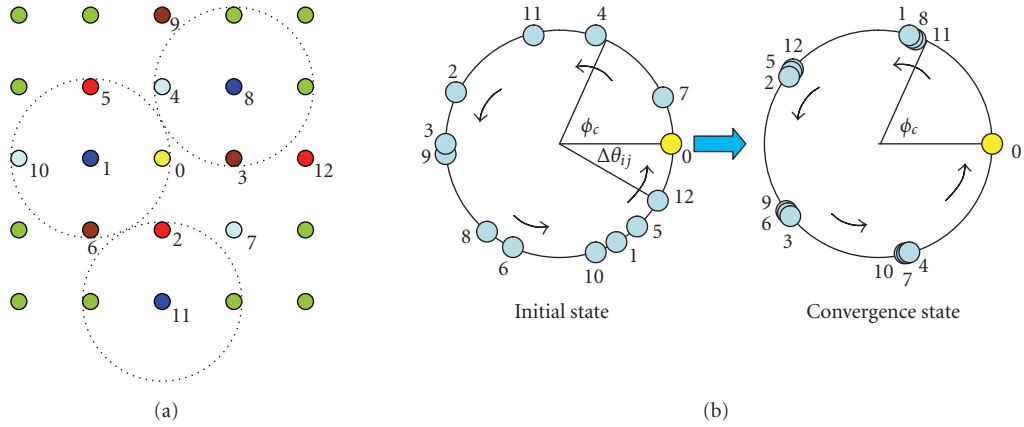

Figure 1: (a) Node arrangement and communication range; (b) phase pattern formation for collision avoidance.

frequent packet collisions. Such collisions should be avoided for not only improvement of the throughput efficiency, but also saving the electric energy consumption required in the retransmissions. Furthermore, several problems are pointed out with regard to the cost of carrier sense [9] and hidden terminals [7, 8]. Also, with the CSMA-based approach, it is difficult to ensure impartial communication right because of the high contention of nodes that share communication channel.

Other research in the wireless sensor networks includes SMAC [10], SMACS [11]. SMAC is based on CSMA, where each node broadcasts a sleep timing schedule to the neighbor nodes. The nodes receiving this message are to adjust the schedule of sleep, by which a node can save energy consumption. Although the problem of collision is inevitable, the aim of this research is focused on a timing control for energy saving. Hence, fundamental problems in CSMA remain unsolved. SMACS realizes an efficient communication based on synchronization between two nodes. These nodes attempt to schedule a communication timing with each other. Additionally, each node utilizes a different frequency band for a different link for collision avoidance. In this method, the risk of collisions can be reduced by random sharing of the frequency band. SMACS is different from the basic TDMA in that synchronization is required between two corresponding nodes while TDMA requires global synchronization. In general, global synchronization without a base station is hard to achieve. We have proposed a distributed communication timing control for collision avoidance named *phase diffusion time-division method* (PDTD) [12]. This method is a distributed communication timing control based on the dynamics of coupled phase oscillator among the peripheral nodes. Through local and fully distributed interactions, the coupled phase dynamics self-organizes the effective phase synchronous state that allows collision-free communication.

On the other hand, radio interference is an important problem in the wireless communication. Interference problems include two kinds of problems. One of them is to reduce influence of interference. Another problem concerns the communication timing under the influence of interference. Radio interference greatly influences the communication protocol [13]. Decentralized scheduling TDMA is based on the graph structure of the node connection within communication range. The issue of radio interference is not considered in decentralized scheduling TDMA. Therefore, in the presence of interference wave, it may not be an appropriate schedule method when considering the issue of interference. Also, in the case of CSMA-based protocol, hidden terminal collision avoidance mechanism based on RTS and CTS messages will not work appropriately [14]. In the previous timing control based on PDTD, we did not deal with radio interference problems. Therefore, unexpected collisions may occur in the real environment. In this paper, we propose the extended version of PDTD with interference detection (PDTD/ID). Each node exchanges the received signal strength and specifies the interference source node. This has to be incorporated for interaction nodes for collision avoidance in PDTD. We verify the efficiency of the proposed method by simulation experiments.

2. COMMUNICATION TIMING CONTROL

2.1. Outline of PDTD

In this section, we will review a basic concept of PDTD. We assume a situation in which a node periodically transmits data. The node is modeled as an oscillator that periodically repeats the states of the communication and noncommunication. Hence, mutual adjustment of the communication timing is formulated based on the coupled oscillator dynamics. The communication timing state of the node is expressed as a phase. The phase of the oscillator for node i is denoted as θ_i, and angular velocity is ω_i. We suppose that each node can transmit data only within the phase interval $0 < \theta_i < \phi_c$ as depicted in Figure 1. If other nodes do not transmit in the interval $0 < \theta_i < \phi_c$, no collision occurs. Figure 1 shows the phase relation from the viewpoint of node 0. Figure 1(left) depicts initial state. In this case, the phase difference is not large enough, hence a collision occurs. If each node forms appropriate communication timing like Figure 1(right), collision does not occur. The node transmits the control message

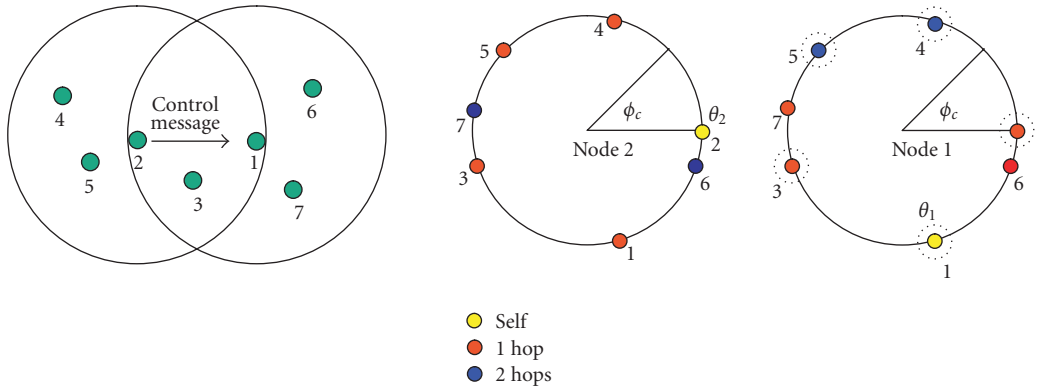

(a) Node arrangement and communication range

(b) Sending phase value by control message

Figure 2: Node interaction based on control message.

at $\theta_i = 0$ for communication timing control. Each node is assumed to know the phase value of the neighbor nodes by receiving the control message, and to calculate phase dynamics.

2.2. Node interaction

We explain the method of exchanging phase value with each other by the control message. The control message from node i includes the following information:

(1) one-hop neighbor node ID $j = (0, 1, 2, \dots)$;
(2) phase value of one-hop neighbor $(\widetilde{\theta}_{i0}, \widetilde{\theta}_{i1}, \widetilde{\theta}_{i2}, \dots, \widetilde{\theta}_{ij})$;
(3) received signal strength value from one-hop neighbor $(P_{i\leftarrow 0}, P_{i\leftarrow 1}, P_{i\leftarrow 2}, \dots, P_{i\leftarrow j})$.

The phase value of one-hop neighbor is used for calculation of communication timing control. The received signal strength value is used for selection of interference nodes. These are detailed in Sections 2.3 and 3. Since the control messages are transmitted by the same channel with the data messages, there is possibility that the control messages might be occasionally lost by collisions. However, the transmission of the control messages is executed periodically, it is unlikely that the control message is lost every time.

The process to convey node information to the neighboring nodes is explained as follows. The node is assumed to be able to know only its self phase value when calculating phase dynamics. However, the node estimates the phase value of the neighboring nodes from their control messages. In this paper, the neighbor node of which information is temporarily generated based on this estimation is called a virtual node. The node controls communication timing by the interaction with a virtual node. Figures 2(a) and 2(b) show the case that node 2 transmits the control message. Figure 2(a) shows node allocation and communication range. Figure 2(b) shows the state of virtual nodes of nodes 1 and 2 corresponding to Figure 2(a). The interaction process of nodes 1 and 2 is as follows. Node 2 transmits the control message at phase $\theta_2 = 0$, then the control message includes information of nodes 1, 3, 4, and 5 that exist in one-hop neighbor. Node 1 that received this massage generates virtual nodes corresponding to nodes 1, 2, 3, 4, and 5 listed in control message from node 2. The phase with dashed circle in Figure 2(b) denotes the corresponding node. A virtual node corresponding to node 2 (sender of the control message) is registered as one-hop neighbor node. Nodes 3, 4, and 5 (the other nodes contained in the control message) are registered as two-hop neighbor nodes. In this regard, node 3 is classified as the two-hop neighbor node from node 1. However, if node 1 is able to communication directly with node 3, node 3 is registered as the one-hop neighbor node. Through sending and receiving of a periodic control message, each node has node information within two-hop neighbor nodes as a virtual node.

2.3. Communication timing control based on PDTD

Coupled phase dynamics

PDTD provides communication timing control based on phase dynamics for collision avoidance. Node i interacts with a virtual node and forms appropriate phase-difference pattern. Let $\widetilde{\theta}_{ij}$ denote phase value of virtual node j for node i. Then the governing equation is given by the following equations:

$$\frac{d\theta_i}{dt} = \omega_i + \sum_{j\in K_i} k_j R(\Delta\widetilde{\theta}_{ij}) + \xi(S_i), \tag{1}$$

$$\Delta\widetilde{\theta}_{ij} = \widetilde{\theta}_{ij} - \theta_i, \tag{2}$$

$$\frac{d\widetilde{\theta}_{ij}}{dt} = \widetilde{\omega}_{ij}, \tag{3}$$

where ω_i and $\widetilde{\omega}_{ij}$ denote the angular velocity of node i and virtual node j, respectively, and k_j is the coupled strength value. K_i is a virtual node set of node i. Every node is allowed to transmit data for $\phi_c/\omega_i(\mathrm{s})$ every cycle. $\xi(S_i)$ is a stochastic term, details of which are explained in Section 2.3. Interaction with the neighbor nodes is governed by phase-response

function $R(\Delta\widetilde{\theta}_{ij})$ which is a repulsive function as follows:

$$R(\Delta\theta_{ij}) = \begin{cases} \Delta\theta_{ij} - \phi_c, & \Delta\theta_{ij} \le \phi_c, \\ 0, & \phi_c < \Delta\theta_{ij} < 2\pi - \phi_c, \\ \Delta\theta_{ij} - 2\pi + \phi_c, & 2\pi - \phi_c \le \Delta\theta_{ij}. \end{cases} \quad (4)$$

Stochastic adaptation

When relying only on the repulsive interaction, the phase-difference pattern often fails to converge to the desired stationary state. Therefore, a stochastic adaptation term $\xi(S_i)$ is introduced, which is determined by the estimated risk of the collision. As an evaluation index, phase overlap rate is defined. Node communication state is defined such that $O_i = 1$ denotes that node i is allowed to communicate, and $O_i = 0$ denotes that node i is prohibited to communicate, which is given by

$$O_i(\theta_i(t)) = \begin{cases} 1, & 0 \le \theta_i < \phi_c, \\ 0, & \phi_c \le \theta_i < 2\pi. \end{cases} \quad (5)$$

Flag function to indicate phase overlap of communication timing between node i and virtual nodes is given by

$$x_i(t) = \begin{cases} 1, & O_i(\theta_i) = 1, \ \sum_{j \in K_i} O_j(\widetilde{\theta}_{ij}) > 0, \\ 0 & \text{else.} \end{cases} \quad (6)$$

$x_i = 1$ indicates that there is a phase overlap that would cause a collision. If $\sum_t^{t+T} x_i(t) \neq 0$, then one collision is counted for one cycle. Let γ indicate the occurrence time of phase overlap for past n cycles. overlap rate c_i is given by

$$c_i(t) = \frac{\gamma}{n}. \quad (7)$$

The stress of being exposed to the risk of collision is accumulated by the following mechanism:

$$S_i(t) = 2S_i(t-\tau) + s(c_i),$$
$$s(c_i) = \begin{cases} 0.0, & 0 \le c_i < 0.2, \\ 0.03, & 0.2 \le c_i < 0.5, \\ 0.05, & 0.5 \le c_i < 0.8, \\ 0.1, & 0.8 \le c_i < 0.9, \\ 0.3, & 0.9 \le c_i, \end{cases} \quad (8)$$

where $\tau = n \cdot T_i$ is a stress accumulating time scale. Random phase jump is implemented every $n \cdot T_i$[s] cycles with probability S_i, where if $S_i > 1$, then $S_i \leftarrow 1$. After random phase jump, then $S_i \leftarrow 0$. The destination of phase jump is decided as follows. Assume that node i has $\widetilde{N}_i$ virtual nodes, the phase of which is denoted as $\widetilde{\theta}_{ij}$. Sorting the phase value $\widetilde{\theta}_{ij}$ in ascending order, such as $\widetilde{\theta}_{il}^{(1)} < \cdots < \widetilde{\theta}_{ij}^{(k)} < \cdots < \widetilde{\theta}_{ik}^{(\widetilde{N}_i)}$, the corresponding node to kth phase value is v_k. The destination of stochastic jump is depicted as shown in Figure 3. The list of destination u_k is given by

$$u_k = \frac{v_k + v_{k+1}}{2} \quad (k = 1, 2, \ldots, \widetilde{N}_i - 1). \quad (9)$$

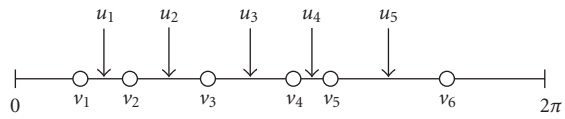

Figure 3: Destination list of random phase jump.

The preferential selection probability u_k is decided by the equation

$$p_k = \frac{\exp(\beta(v_{k+1} - v_k))}{\sum_{l=1}^{\widetilde{N}_i - 1} \exp(\beta(v_{l+1} - v_l))} \quad (l = 1, 2, \ldots, \widetilde{N}_i - 1), \quad (10)$$

where β is a sensitivity parameter of the selection.

3. COMMUNICATION TIMING CONTROL WITH INTERFERENCE NODE DETECTION

3.1. Radio interference problem

In a wireless communication, even in the presence of weak interference wave, a node may fail to communicate if the desired wave strength from the node is weak. On the other hand, if the desired wave strength is sufficiently strong, the node may be able to receive data from the other node successfully despite presence of a strong interference wave. The reception error caused by an interference wave is estimated by signal-to-interference ratio (SIR). The threshold of SIR to correctly receive a signal is determined by modulation methods and spec of the receiver. In the communication timing control described in Section 2.3, however, the influence of interference wave was not taken into account in our model. In spite of the assumption that the interaction range is within the two-hop neighbors, interference waves can be reached beyond the interaction range, and hence this could cause unexpected collisions. Therefore, each node has to select the interaction nodes based on the relation between received signal wave strength and interference wave strength.

3.2. Radio interference model

In this section, we discuss how the interference source is specified based on the received electric power. As shown in Figure 4, nodes i, j, and k are placed, where the internode distance between nodes i and j and the one between nodes j and k are denoted by d_s, d_i, respectively. The interference occurs in node j when node i transmits to node j. Also assume that all nodes transmit in the same electric power t_p(mW). The received electric power $p(d)$(mW) is assumed available by the following equation [14]:

$$p(d) = \frac{c \cdot t_p}{d^{\alpha}}, \quad (11)$$

where d is the distance between the sender node and the receiver node. α is the signal attenuation coefficient. c is the combined parameter that is related to the reception strength. Assume that node i is the transmitting source, and node k is

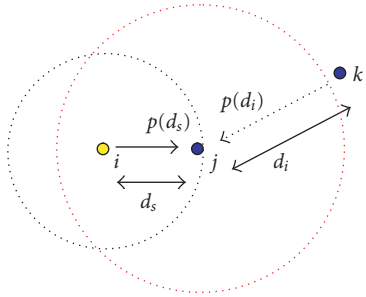

Figure 4: The existence range of interference source (ERIS).

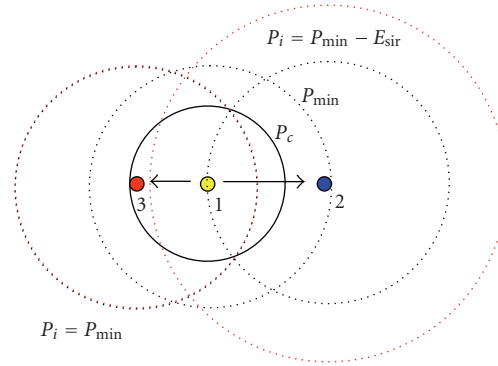

Figure 5: Limitation of destination node and ERIS.

an interference source. With (11), SIR is defined as the ratio of the electric power between the desired signal from node i and the interference wave from node k;

$$\mathrm{SIR} = \frac{p(d_s)}{p(d_i)} = \left(\frac{d_i}{d_s}\right)^{\alpha}. \tag{12}$$

SIR has to be bigger than the threshold e_{sir} in order for the transmission from node i to be successfully received in node j. Otherwise, in the case of SIR $\leq e_{\mathrm{sir}}$, the interference would occur in node j, and node k is referred to as the interference source node for node j. In general, the existence range of interference source node is given by the following equation:

$$d_i \leq \sqrt[\alpha]{e_{\mathrm{sir}}}\, d_s. \tag{13}$$

We call the existence range of interference source node as ERIS in the following section. It can be said that ERIS is proportional to the distance d_s by (13). In order for node i to be able to communicate with node j successfully, node i has to specify which node can be the interference node for node j. Such nodes are referred to as the interference source nodes. Node i is not allowed to transmit at the same time as the interference source node.

3.3. Interference node detection

Existence range of interference source

As mentioned in the previous section,

$$\mathrm{SIR} = \frac{p(d_s)}{p(d_i)} > e_{\mathrm{sir}} \tag{14}$$

is required for successful communication in the presence of interference waves. Taking logarithm in (14), we obtain

$$P_s - P_i > E_{\mathrm{sir}}, \tag{15}$$

where $P_s = 10\log_{10} p(d_s)$, $P_i = 10\log_{10} p(d_i)$, and $E_{\mathrm{sir}} = 10\log_{10} e_{\mathrm{sir}}$. Figure 5 shows the existence range of interference source (ERIS). Let P_{min}(dBm) be the minimum received signal strength for a successful communication. In the case that node 1 transmits to node 2 that is located on the boundary of communication range from node 1, the received signal strength on the boundary positions will become P_{min}(dBm). Hence, it is supposed that $P_s = P_{\mathrm{min}}$ in (15), then $P_{\mathrm{min}} - E_{\mathrm{sir}} > P_i$ is derived, which indicates that node 2 will fail to receive the transmission from node 1, if the strength of interference wave is larger than $P_i = P_{\mathrm{min}} - E_{\mathrm{sir}}$(dBm). The ERIS, the corresponding range for P_i, will become larger than the communication range of node 2. Therefore, some extension is required for the timing control with two-hop neighbor nodes based on the PDTD because the interference wave may cause another collision. On the other hand, when node 1 transmits to node 3, which is closer than node 2, assume that node 3 receives the signal of strength $P_c = P_{\mathrm{min}} + E_{\mathrm{sir}}$(dBm). This is the case of $P_s = P_c$ in (15), where since $P_c - E_{\mathrm{sir}} > P_i$, $P_{\mathrm{min}} > P_i$ is obtained. This implies that the ERIS (P_i) is the same or inside of the communication range of node 3. Therefore, if the communication range is redefined as P_c instead of P_{min}, it is possible to avoid the problem caused by the interference wave in PDTD.

Detection process of interference node

In this section, the process of interference node detection is addressed. This method is based on the evaluation of the received signal strength, where two different scenarios can be considered. The first case is that when node a transmits to node b, the interference occurs in the destination node b because of transmissions from some other nodes. In this case, node a needs to specify which nodes are causing the interference to node b (detection of the interference nodes), in an attempt to execute the timing control with such interference nodes. On the other hand, the second case is that the transmission from node a to a destination node c is causing an interference to node b, where node a is becoming an interference node for node b unintentionally, and such a node could exist many around node a. Hence, node a is asked to specify the node set that can be interfered by the transmission of node a, and conduct a timing control with those nodes to avoid a potential collision.

The first case is exemplified in more detail in Figure 6(a), where node 1 receives a control message from node 2 with the signal strength larger than P_c(dBm) in an attempt to

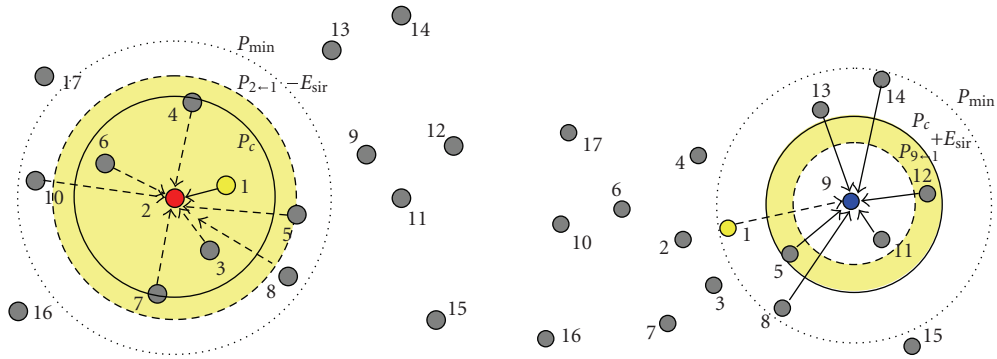

(a) A case that node 1 receives control message from node 2 with signal strength larger than P_c(dBm)

(b) A case that node 1 receives control message from node 9 with signal strength less than P_c(dBm)

Figure 6: Interference node selection based on received signal strength.

specify the interference nodes for node 2. As described in Section 2.2, the control message from node 2 includes the signal strength data which had been received by node 2 from the other nodes. In Figure 6(a), this control message includes data from nodes 1, 3, 4, 5, 6, 7, 8, and 10.

Let $P_{b\leftarrow a}$ denote the received signal strength of node b from node a, then node 1 compares $P_{2\leftarrow 1}$ (the desired signal) with $P_{2\leftarrow x}$, $(x = 3, 4, 5, 6, 8, 10)$ in order to judge as to whether each node x would become the interference source. From (15), if $P_{2\leftarrow 1} - P_{2\leftarrow x} \leq E_{\text{sir}}$, node x may cause the interference to node 2. Such a node set is defined as

$$L_I(b \longleftarrow a) = \{x \mid P_{b\leftarrow x} \geq P_{b\leftarrow a} - E_{\text{sir}},\ x \neq a\}. \quad (16)$$

Equation (16) represents the node set that could cause the interference to node b when node a transmits to node b. It should be noted that the node set $L_I(b \leftarrow a)$ is determined by node a based on the control message from node b, hence node a is excluded from the set $L_I(b \leftarrow a)$. As depicted in Figure 6(a), $L_I(2 \leftarrow 1) = \{3, 4, 5, 6, 7\}$ that are the nodes inside the range of dashed circle, $P_{2\leftarrow 1} - E_{\text{sir}}$. While, the second scenario is exemplified in Figure 6(b) where there is no direct communication between nodes 1 and 9 but node 1 can receive the control message from node 9 with the signal strength of less than P_c(dBm) for the sake of the interaction in PDTD. In other words, node 1 is outside the communication range P_c though it is within the interaction range $P_{\min}$. Node 9 will have a direct communication with node x, the signal strength of which is $P_{9\leftarrow x} > P_c$. When node 1 transmits to a peripheral node, such as node 2, the transmission from node 1 may interfere with the desired signal for node 9 from node x, for instance, $x = 12$. Also, if $P_{9\leftarrow x} - P_{9\leftarrow 1} \leq E_{\text{sir}}$ holds, node 1 becomes an interference node to the desired signal for node 9. Therefore, the node set comprising the nodes that are interfered with the transmission of node A and prevented from receiving a desired signal from node B is defined as follows:

$$C_I(b \longleftarrow a) = \{x \mid P_{b\leftarrow x} \leq P_{b\leftarrow a} + E_{\text{sir}},\ P_{b\leftarrow x} \geq P_c,\ x \neq a\}. \quad (17)$$

It should be noted that since $C_I(b \leftarrow a)$ is estimated by node a based on the received control message from node b, node a is excluded from the node set $C_I(b \leftarrow a)$. As an example, $C_I(9 \leftarrow 1) = \{5, 12\}$ is depicted in the confined colored area of Figure 6(b).

In this method, the parameters associated with necessary SIR threshold E_{sir} and the minimum reception electric power $P_{\min}$ have to be preassigned in order to abstract the interference nodes. After every node specifies the interference nodes, it conducts a communication timing control with those included in L_I and C_I. That is, the interaction nodes (the virtual node set for node i) K_i in (1) are adaptively specified as $L_I(j \leftarrow i) \cup C_I(j \leftarrow i)$.

4. SIMULATION

4.1. Simulation setting

Simulations are conducted to illustrate performance of PDTD/ ID. As a simulation setting, 10×10 nodes are assigned as follows.

Case 1 (regular grid model (Figure 7(a))). 10×10 nodes are assigned on the regular grid, where the internode distance is assumed as $d = 25$ (m).

Case 2 (perturbed grid model (Figure 7(b))). Node allocation is perturbed by the uniform random value in $[-d/2, d/2)$ from the regular grid allocation.

The radio parameters and the node parameters are listed in Tables 1 and 2, respectively. Also, the node arrangement and communication range are depicted in Figure 7. The initial value of the phase θ_i is randomly assigned in $[0, 2\pi)$ for both Cases 1 and 2. Since the purpose of this simulation is to verify the proposed timing control and interference node selection, we focus our argument on the timing control, hence the traffic model is simplified. Each node transmits packets in the phase interval $0 < \theta_i < \phi_c$ every cycle. It is preferable that the node decides ϕ_c as autonomous. However, we decide ϕ_c

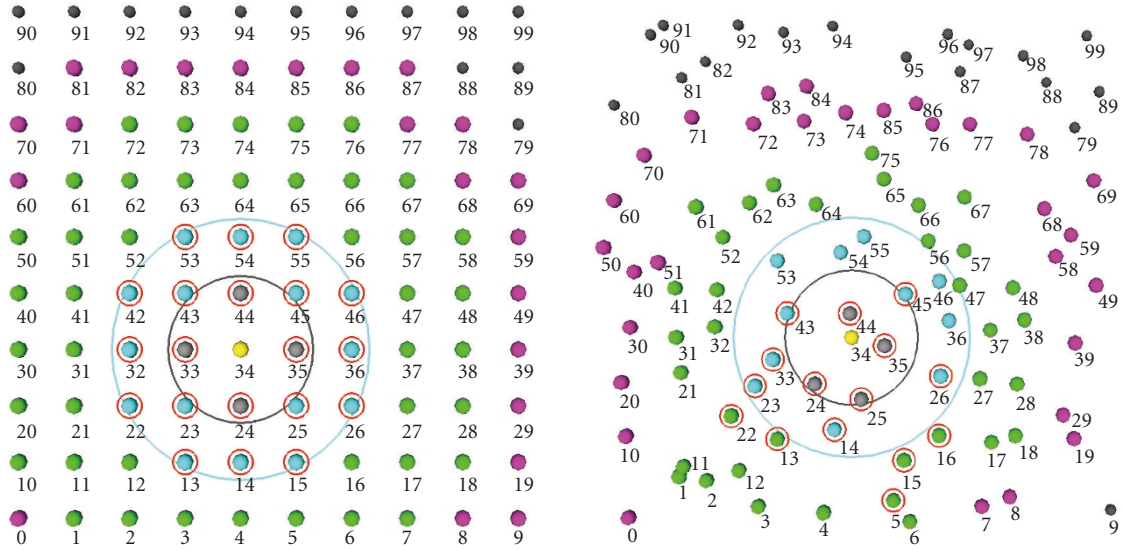

(a) Regular grid (b) Perturbed grid

Figure 7: Node arrangement and interference node.

Table 1: Radio parameters.

$c \cdot p_t$	Radio parameter	0.01135
α	Signal attenuation coefficient	4
E_{sir}	Necessary SIR	10 (dB)
P_{min}	Lowest reception electric power	−90 (dBm)

Table 2: Node parameters.

ϕ_c	Available communication interval	$2\pi/15$ (Case 1) (rad) $2\pi/27$ (Case 2 with ID) (rad) $2\pi/34$ (Case 2 w/o ID) (rad)
n	Calculation cycle of collision rate	5 cycles
ω	Eigenfrequency of node	$2\pi/5$ (rad/s)
β	Sensitivity of stochastic jump	10

as a fixed value in this simulation. We evaluate the successful transmission rate that is defined as available communication time(s) per cycle normalized by the maximum communication time(s) per cycle (ϕ_c/ω_i). Collision rate is the collision state time(s) per cycle normalized by the maximum communication time(s) per cycle.

4.2. Simulation results

The results of node selection for interaction are shown in Figures 7(a) and 7(b), where the large circle indicates the communication range of node 34, and the small circle indicates the equivalent curve of the signal strength P_c from node 34. The encircled nodes in Figure 7 imply the interference nodes in the case that node 34 transmits to a node within the small circle P_c curve (or communication range); hence node 34 has to interact with encircled nodes for collision avoidance. Table 3 shows a specific example for signal strength values in the case of Figure 7(b). Table 3(a) shows the list of signal strength in the case that node 34 receives the control message from node 35, the information gathered by node 35. Node 34 specifies the interaction nodes based on (16). Because the value of SIR is less than the desired threshold $E_{\text{sir}} = 10$ (dB) as listed in Table 1 for successful reception, node 34 has to avoid the overlap of communication timing with nodes 25, 44, and 45. Table 3(b) shows the table of signal strength, when node 34 receives a control message from node 33, and node 34 selects interaction node based on (17). Because node 34 interferes with reception of node 33, node 34 has to avoid overlap of communication timing with 24 and 43. Thus, interaction nodes (encircled nodes in Figure 7) are selected autonomously.

As mentioned in Section 2.3, each node evaluates the overlap rate of communication phase by (7). It can be said that the phase-difference pattern for the communication timing control is completed when the overlap rate of all nodes converged to 0. The time series of average overlap rate is shown in Figures 8(a) and 9(a), and it can be seen that it took around 60–100 cycles to complete the timing control. Also, average successful transmission rate increased according to decline of the average overlap rate as shown in Figures 8(b) and 9(b). Because of the overhead of the control message for interactions, the average success transmission rate is inevitably below 1. After having converged to the stationary state, the successful transmission rate remained steady in the high value, and any collision did not occur as shown in Figures 8(c) and 9(c). Hence, it is confirmed that every node correctly specified the interference source nodes and effectively conducted the communication timing control with interaction nodes. During the timing formation, it was possible

Table 3: Signal strength and interaction node selection.

(a) Control message from 35, receiver node 34, corresponding to Figure 7(b)

$P_{b\leftarrow a}$	Strength (dBm)	SIR (dB)
$P_{35\leftarrow 34}$	−68.3	Desired wave
$P_{35\leftarrow 14}$	−86.5	18.2
$P_{35\leftarrow 15}$	−89.5	21.2
$P_{35\leftarrow 16}$	−87.8	19.5
$P_{35\leftarrow 24}$	−83.1	14.8
$P_{35\leftarrow 25}$	−77.5	9.2°
$P_{35\leftarrow 26}$	−79.2	10.9
$P_{35\leftarrow 27}$	−87.2	18.9
$P_{35\leftarrow 33}$	−89.2	20.9
$P_{35\leftarrow 36}$	−80.7	12.4
$P_{35\leftarrow 37}$	−88.2	19.9
$P_{35\leftarrow 43}$	−87.5	19.2
$P_{35\leftarrow 44}$	−74.0	5.7°
$P_{35\leftarrow 45}$	−76.8	8.5°
$P_{35\leftarrow 46}$	−84.1	15.8
$P_{35\leftarrow 47}$	−86.4	18.1
$P_{35\leftarrow 54}$	−87.5	19.2
$P_{35\leftarrow 55}$	−88.7	20.4
$P_{35\leftarrow 56}$	−89.1	20.8

(b) Control message from 33, receiver node 34, corresponding to Figure 7(b)

$P_{b\leftarrow a}$	Strength (dBm)	SIR (dB)
$P_{33\leftarrow 34}$	−83.6	Interference wave
$P_{33\leftarrow 12}$	−89.5	Out of P_c
$P_{33\leftarrow 13}$	−82.9	Out of P_c
$P_{33\leftarrow 14}$	−85.8	Out of P_c
$P_{33\leftarrow 21}$	−85.8	Out of P_c
$P_{33\leftarrow 22}$	−80.8	Out of P_c
$P_{33\leftarrow 23}$	−67.2	16.9
$P_{33\leftarrow 24}$	−74.5	9.1°
$P_{33\leftarrow 25}$	−86.5	Out of P_c
$P_{33\leftarrow 31}$	−87.0	Out of P_c
$P_{33\leftarrow 32}$	−80.0	Out of P_c
$P_{33\leftarrow 35}$	−89.1	Out of P_c
$P_{33\leftarrow 42}$	−85.0	Out of P_c
$P_{33\leftarrow 43}$	−74.3	9.3°
$P_{33\leftarrow 44}$	−85.1	Out of P_c
$P_{33\leftarrow 53}$	−86.7	Out of P_c

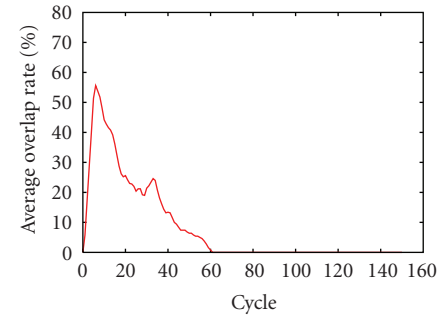

(a) Average overlap rate

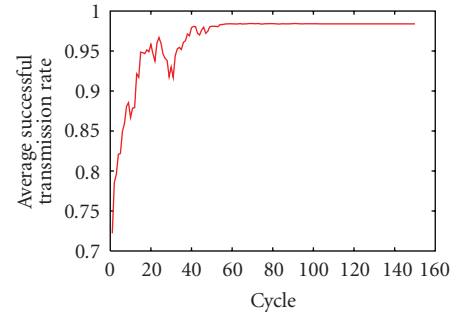

(b) Average successful transmission rate

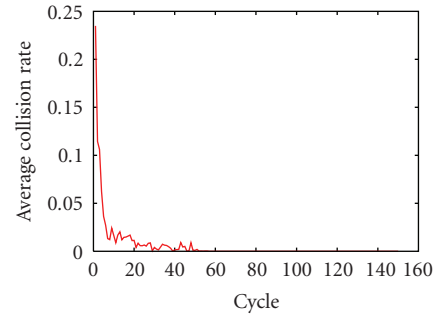

(c) Average collision rate

Figure 8: Simulation result in Case 1.

to keep the collision rate at low level by collision avoidance based on the exchange of the communication timing information. Average collision rate declined sharply as shown in Figures 8(c) and 9(c).

Figure 9 shows performance difference with/without interference node detection. In the case without interference node detection, in spite of phase overlap rate becomes 0, average collision rate indicates 0.1. That collision is caused by influence of nodes outside two hops. Additionally, available phase interval ϕ_c becomes small (with ID $2\pi/27$, without ID $2\pi/34$) so that a lot of interaction nodes exist. However, interference node detection has the limitation of range of destination node (Figure 5).

Figures 10(a) and 10(b) show the spatial distribution of the successful transmission rate and the collision rate. After having completed the timing control, the inequality of transmission right was prevented. In the conventional contention-based access control, the equal transmission right is difficult to achieve. Thus, the communication timing control which can also cope with the interference wave is realized in a static radio condition. However, the reception signal strength may change dynamically due to the influence of fading effect, a problem remaining to be dealt with in our future work.

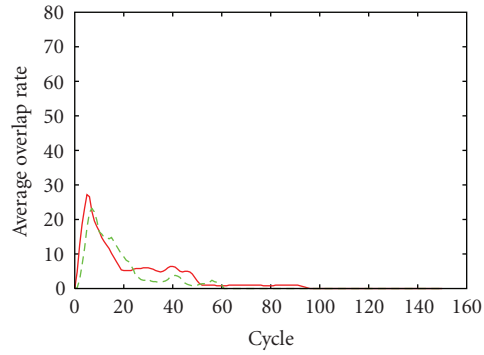

(a) Average overlap rate

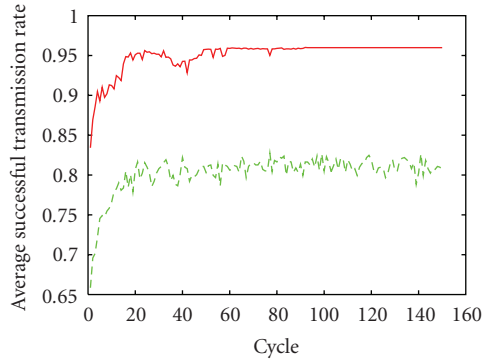

(b) Average successful transmission rate

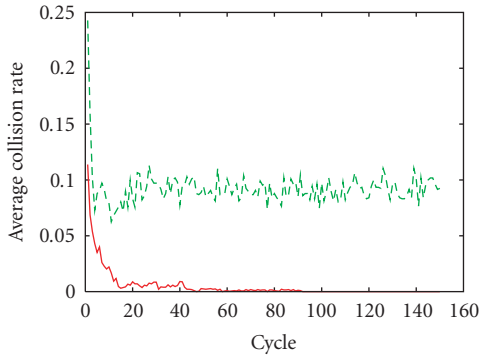

(c) Average collision rate

FIGURE 9: Simulation result in Case 2 (performance difference with/without interference detection).

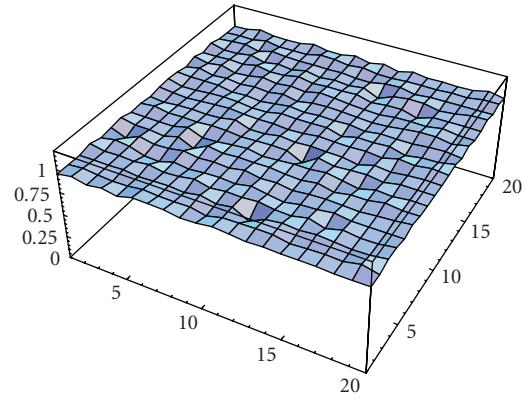

(a) Average time of successful transmission rate

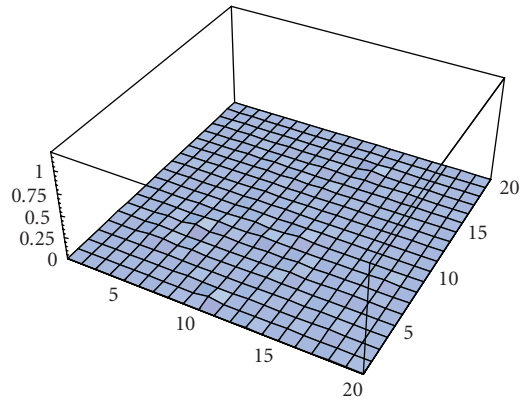

(b) Average time of collision rate

FIGURE 10: Spatial distribution of successful transmission rate and collision rate.

5. CONCLUSION

In this paper, we proposed a novel communication timing control method for the wireless networks, named *phase diffusion time-division method with interference detection*, PDTD/ID. Without interference detection, PDTD may be faced with difficulty to operate in real environment. Through the local exchanging of received signal strength value, every node selects the interaction nodes for collision avoidance in the presence of interference wave. PDTD/ID realizes a fully distributed timing control with the interference node detection. A model of the interference wave was examined for the simulation, and the simulation experiments illustrated satisfactory results in the large-scale network. Interaction node selecting method based on the reception signal strength is expected to be effective in the real environment.

REFERENCES

[1] I. F. Akyildiz, W. Su, Y. Sankarasubramaniam, and E. Cayirci, "Wireless sensor networks: a survey," *Computer Networks*, vol. 38, no. 4, pp. 393–422, 2002.

[2] D. D. Falconer, F. Adachi, and B. Gudmundson, "Time division multiple access methods for wireless personal communications," *IEEE Communications Magazine*, vol. 33, no. 1, pp. 50–57, 1995.

[3] A. Ephremides and T. V. Truong, "Scheduling broadcasts in multihop radio networks," *IEEE Transactions on Communications*, vol. 38, no. 4, pp. 456–460, 1990.

[4] C. D. Young, "USAP multiple access: dynamic resource allocation for mobile multihop multichannel wireless networking," in *Proceedings of IEEE Military Communications Conference (MILCOM '99)*, vol. 1, pp. 271–275, Atlantic City, NJ, USA, October-November 1999.

[5] M. K. Marina, G. D. Kondylis, and U. C. Kozat, "RBRP: a robust broadcast reservation protocol for mobile ad hoc networks," in *Proceedings of IEEE International Conference on Communications (ICC '01)*, vol. 3, pp. 878–885, Helsinki, Finland, June 2001.

[6] Z. Tang and J. J. Garcia-Luna-Aceves, "A protocol for topology-dependent transmission scheduling in wireless networks," in *Proceedings of IEEE Wireless Communications and Networking Conference (WCNC '99)*, vol. 3, pp. 1333–1337, New Orleans, La, USA, September 1999.

[7] L. Kleinrock and F. Tobagi, "Packet switching in radio channels: part I—carrier sense multiple-access modes and their throughput-delay characteristics," *IEEE Transactions on Communications*, vol. 23, no. 12, pp. 1400–1416, 1975.

[8] F. Tobagi and L. Kleinrock, "Packet switching in radio channels: part II—the hidden terminal problem in carrier sense multiple-access and the busy-tone solution," *IEEE Transactions on Communications*, vol. 23, no. 12, pp. 1417–1433, 1975.

[9] S. G. Glisic, "1-persistent carrier sense multiple access in radio channels with imperfect carrier sensing," *IEEE Transactions on Communications*, vol. 39, no. 3, pp. 458–464, 1991.

[10] W. Ye, J. S. Heidemann, and D. Estrin, "An energy-efficient MAC protocol for wireless sensor networks," in *Proceedings of 21st Annual Joint Conference of the IEEE Computer and Communications Societies (INFOCOM '02)*, pp. 1567–1576, New York, NY, USA, June 2002.

[11] K. Sohrabi, J. Gao, V. Ailawadhi, and G. J. Pottie, "Protocols for self-organization of a wireless sensor network," *IEEE Personal Communications*, vol. 7, no. 5, pp. 16–27, 2000.

[12] K. Sekiyama, Y. Kubo, S. Fukunaga, and M. Date, "Distributed time division pattern formation for wireless communication networks," *International Journal of Distributed Sensor Networks*, vol. 1, no. 3-4, pp. 283–304, 2005.

[13] J. Li, C. Blake, D. S. J. De Couto, H. I. Lee, and R. Morris, "Capacity of ad hoc wireless networks," in *Proceedings of the 7th ACM International Conference on Mobile Computing and Networking*, pp. 61–69, Rome, Italy, July 2001.

[14] F. Ye, S. Yi, and B. Sikdar, "Improving spatial reuse of IEEE 802.11 based ad hoc networks," in *Proceedings of IEEE Global Telecommunications Conference (GLOBECOM '03)*, vol. 2, pp. 1013–1017, San Francisco, Calif, USA, December 2003.